Rapid Delivery of Nanobodies/V$_H$Hs into Living Cells via Expressing *In Vitro*-Transcribed mRNA

Xuechen Zhou,[1] Rui Hao,[1] Chen Chen,[1] Zhipeng Su,[1] Linhong Zhao,[1] Zhuojuan Luo,[1] and Wei Xie[1]

[1]The Key Laboratory of Developmental Genes and Human Disease, School of Life Science and Technology, Southeast University, 2 Sipailou Road, Nanjing 210096, China
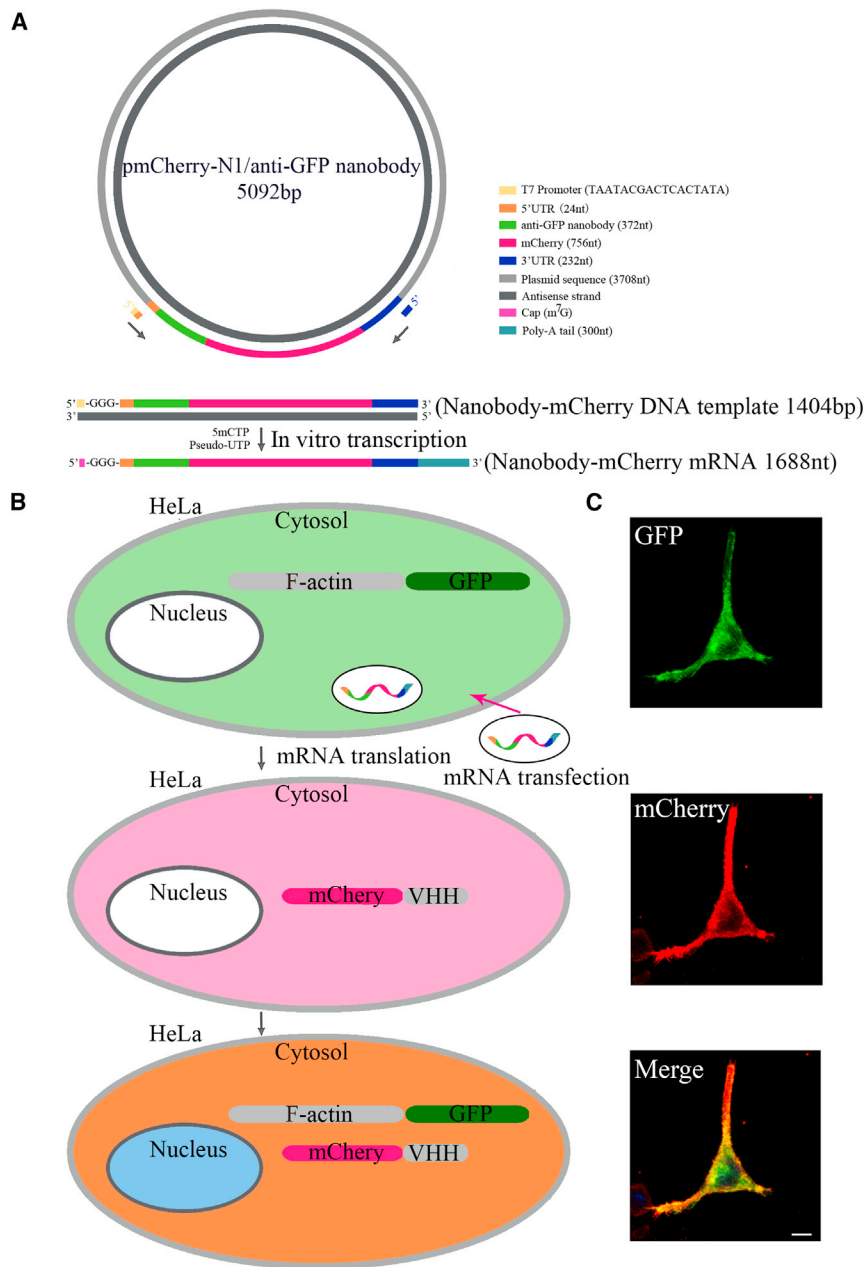
Intracellular antigen labeling and manipulation by antibodies have been long-thought goals in the field of cell research and therapy. However, a central limitation for this application is that antibodies are not able to penetrate into the cytosol of living cells. Taking advantages of small sizes and unique structures of the single-domain antibodies, here, we presented a novel approach to rapidly deliver the nanobody/variable domain of heavy chain of heavy-chain antibody (V$_H$H) into living cells via introducing its coding mRNA, which was generated by *in vitro* transcription. We demonstrated that actin-green fluorescent proteins (GFP) and Golgi-GFP can be recognized by the anti-GFP nanobody/V$_H$H, vimentin can be recognized by the anti-vimentin nanobody/V$_H$H, and histone deacetylase 6 (HDAC6) can be recognized by the anti-HDAC6 nanobody/ V$_H$H, respectively. We found that the anti-GFP nanobody expressed via *in vitro*-transcribed (IVT) mRNA can be detected in 3 h and degraded in 48 h after transfection, whereas the nanobody expressed via plasmid DNA, was not detected until 24 h after transfection. As a result, it is effective in delivering the nanobody through expressing the nanobody/V$_H$H in living cells from its coding mRNA.

INTRODUCTION

Over the past decades, tremendous progress has been made in modifying conventional antibodies to variable forms of antibodies in different structures and sizes,[1] and now antibodies are widely used from basic lab research to medical therapies.[2–4] However, a major limitation is that conventional antibodies are not able to penetrate into living cells, since the high molecular weight of antibodies prevents them from crossing the cell membranes to access intracellular targets.[5,6] Up to now, there are four major approaches to deliver antibodies into living cells, including intrabodies, protein transfection (profection), peptides as protein transduction domains (transmabs/transbodied), and fusion to targeting proteins. Antibodies delivered using the above approaches usually bear a cytosol-penetrating ability.[7]

Developing antibodies in a smaller size is a fundamental problem in this field. The antigen-binding fragment (Fab) of a heavy-chain antibody, which is devoid of light chains and recognizes antigens via their variable domain from Camelidae sp. (referred to as variable domain of heavy chain of heavy-chain antibody (V$_H$H) or nanobody),

represents the smallest intact antigen-binding fragment.[8–10] Nanobodies/V$_H$Hs are small (13–14 kDa) antibody fragments that consist of just one variable heavy-chain domain of a heavy-chain antibody.[11] To date, the most advanced method in delivering antibodies to the endoplasmic reticula (ERs) is transfection with a plasmid-containing coding sequence of nanobodies/V$_H$Hs.[12] However, as recombinant plasmid transfection is associated with multiple serious safety issues, this approach is still limited to research purposes.

In vitro-transcribed (IVT) mRNA is an ideal carrier to deliver genetic information into living cells.[13] Over the last years, many interesting techniques of IVT mRNA were proposed and shown to be useful for many applications. So the development of IVT mRNA-based therapeutics has gained broad attention.[14] One of the main uses of IVT mRNA is to deliver protein into living cells, but recently, nanobodies/V$_H$Hs have been expanded toward mining from traditional antibodies.

Since the foundations of nanobodies/V$_H$Hs transfected into living cells, as well as the burst of IVT mRNA, the problem of nanobodies/V$_H$Hs expressed with high efficiency and safety has been in a scope of interest of numerous researchers from this field. Here, we focus only on transferring the nanobody/V$_H$H targeting cell skeletons, organelle, or other cytoplasmic molecules via expressing its IVT mRNA. We chose an anti-green fluorescent protein (GFP) nanobody/V$_H$H sequence (CAN 375),[10,15] anti-vimentin nanobody/V$_H$H sequence (CAN 2391),[10,16] as well as anti-histone deacetylase 6 (HDAC6) nanobody/V$_H$H sequence (unpublished) expressed via IVT mRNAs and studied their distribution in cells. Also, we investigated how the stability of IVT mRNA is regulated. Moreover, we compared the relative fluorescence intensity of the anti-GFP nanobody/V$_H$H, expressed via IVT mRNA and via plasmid, including production and degradation. Our study suggests a potential strategy to expand the applications of the nanobody/V$_H$H via expressing its IVT mRNA in living cells.

structed GFP-binding nanobody/V$_H$H expressed in the form of RNA instead of DNA, termed as nanobody-mCherry expressed via IVT mRNA. We quickly produced anti-reverse cap analog (ARCA)-capped and poly(A)-tailed mRNA with untranslated regions (UTRs) and chemically modified nucleotides *in vitro*. The mRNA synthesized with the kit can be used for transfection (Figures 1A and 1B).

We then investigated the ability of the anti-GFP nanobody-mCherry expressed via IVT mRNA in accessing and binding its epitopes in living cells. To test the expression of the anti-GFP nanobody/V$_H$H in living cells, we fused it to mCherry to generate a "visible" anti-GFP antibody. Actin is a typical epitope in the cytoplasm, which is incorporated into growing actin filaments and can be visualized directly. Thus, we cotransfected HeLa cells with the filamentous actin (F-actin)-GFP expression construct and the nanobody-mCherry expressed via IVT mRNA. A representative confocal image of a double-transfected cell showed green and red fluorescence at the cytoskeleton (Figure 1C), which is indicative of correct incorporation of F-actin-GFP into the actin filaments and efficient recognition by the nanobody-mCherry expressed via IVT mRNA. The green field represented GFP, which was coexpressed with F-actin, and the red field represented mCherry, which was coexpressed with the nanobody/

V$_H$H. Double-immunofluorescent development revealed colocalization of F-actin and the nanobody/V$_H$H in HeLa cells.

RESULTS

Illustration and Characterization of the Anti-GFP Nanobody/V$_H$H Expressed via the IVT mRNA Concept

Most nanobodies/V$_H$Hs can be functionally expressed as intrabodies via plasmids transfected into a eukaryotic cell. This makes nanobodies/V$_H$Hs ideal tools to recognize structural or dynamic features observed by biochemical measurements in living cells. Previous reports have indicated that the epitope-recognizing fragment of heavy-chain antibodies from Camelidae sp. with fluorescent proteins to generate fluorescent, antigen-binding nanobodies/V$_H$Hs (chromobodies)[12] can be expressed in living cells via plasmid transfection. Here, we con-

Nanobodies/V$_H$Hs Expressed via IVT mRNAs Recognizing Specific Cytoplasmic Antigens in Living Cells

We cotransfected the F-actin-GFP expression construct with the anti-GFP nanobody-mCherry expressed via IVT mRNA into A549 cells. We also cotransfected the Golgi-GFP expression construct with the nanobody-mCherry expressed via IVT mRNA into HeLa cells and analyzed them by live cell microscopy (Figures 2A and 2B). As a result, the nanobody-mCherry expressed via IVT mRNA was
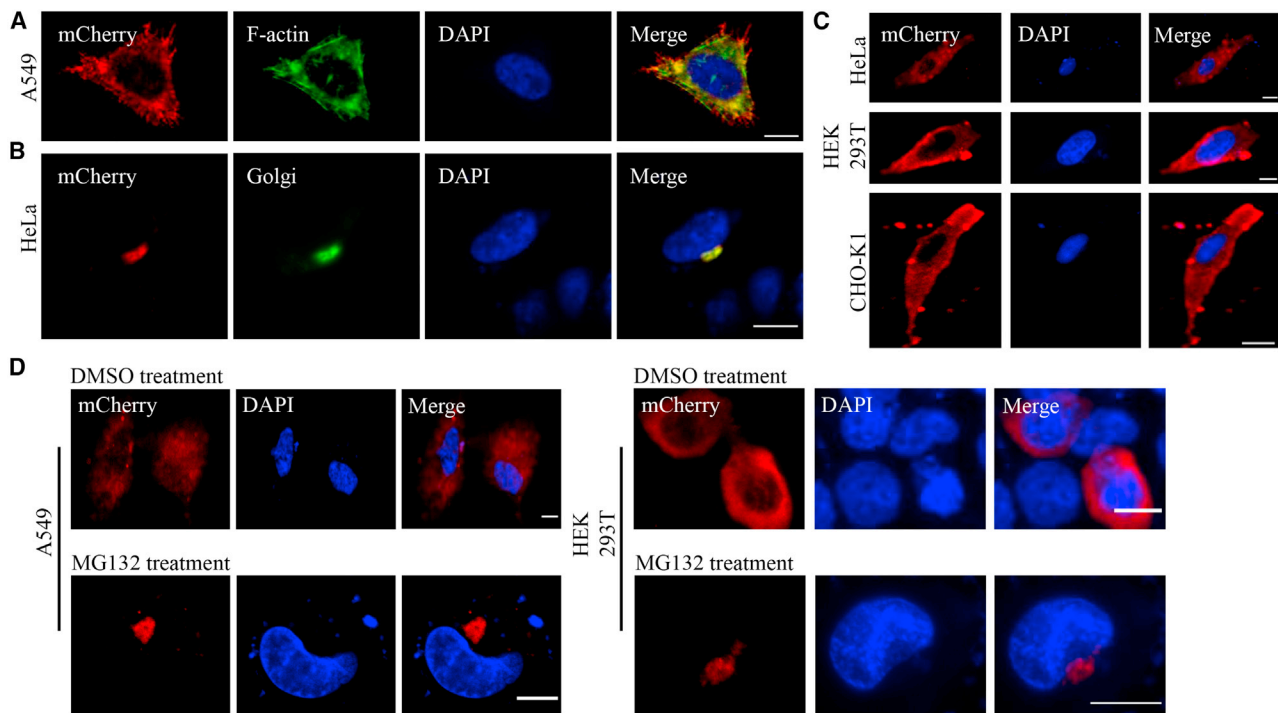
Figure 2. Nanobodies/V$_H$Hs Expressed via IVT mRNAs Recognizing Specific Cytosol Antigens in Living Cells

(A) Anti-GFP nanobody-mCherry expressed via IVT mRNA recognizes F-actin-GFP in A549 cells. (B) Anti-GFP nanobody-mCherry expressed via IVT mRNA recognizes Golgi-GFP in HeLa cells. (C) Anti-vimentin nanobody-mCherry expressed via IVT mRNA recognizes vimentin in cytoplasm in HeLa, HEK293T, and CHO-K1 cells. (D) A549 and HEK293T cells were treated with DMSO or 2 μM MG132 for 24 h and then sequentially incubated with the anti-HDAC6 nanobody-mCherry expressed via IVT mRNA. The nanobody/V$_H$H recognizes HDAC6 within the inclusion body in cytoplasm in A549 and HEK293T cells after MG132 treatment. Confocal midsections of living cells are shown. Scale bars, 10 μm.

successfully generated, which can bind F-actin and Golgi in A549 and HeLa cells, respectively.

Vimentin is the major intermediate filament of mesenchymal cells and is mainly involved in tissue integrity and cytoarchitecture.[17] HeLa, HEK293T, and Chinese hamster ovary (CHO)-K1 cells were transfected with the IVT mRNA coding anti-vimentin nanobody-mCherry and analyzed by live cell microscopy (Figure 2C). As a result, the anti-vimentin nanobody-mCherry expressed via IVT mRNA was successfully generated and can be distributed in cytoplasm mainly, not shown in the cell nucleus.

HDACs are enzymes that catalyze the removal of acetyl groups from the lysine residues located on histone and nonhistone proteins. HDAC6 is a cytoplasmic enzyme that uniquely features two catalytic domains. HDAC6 is a component of aggresome,[18] which could be induced by the proteasome inhibitor MG132.[19] A549 and HEK293T cells were transfected with the IVT mRNA coding anti-HDAC6 nanobody-mCherry and analyzed by live cell microscopy (Figure 2D). As a result, the anti-HDAC nanobody-mCherry expressed via IVT mRNA was successfully generated, can recognize HDAC6 within the inclusion body in cytoplasm after MG132 treatment, and can be distributed in cytoplasm mainly after DMSO treatment as compared.

Thus, the nanobodies/V$_H$Hs expressed via IVT mRNAs were strongly expressed and can recognize antigens of cell skeletons, organelle, and cytosol in different kinds of living cells. The distribution of nanobodies presented structures in shapes of the cell skeleton or the Golgi.

The Anti-GFP Nanobody-mCherry Expressed via IVT mRNA Produced and Degraded Earlier Than the pmCherry-N1/ Nanobody

To accelerate the production and increase the transfection efficiency of nanobody-mCherry, HeLa cells were transfected with the same concentration of the IVT mRNA and pmCherry-N1/anti-GFP nanobody. Western blot and microscopy analyses of transfected cells showed that the anti-GFP nanobody-mCherry expressed via IVT mRNA can be expressed at 3 h after transfection, whereas the nanobody-mCherry expressed via the plasmid was not expressed until 24 h after transfection (Figures 3A and 3B).

Furthermore, the existing of DNA in cell lines may expose a risk of genome integration and cause multiple serious safety issues. The nanobody-mCherry expressed via IVT mRNA peaked at 24 h after transfection and then degraded quickly. At 72 h after transfection, the nanobody-mCherry expressed via IVT mRNA
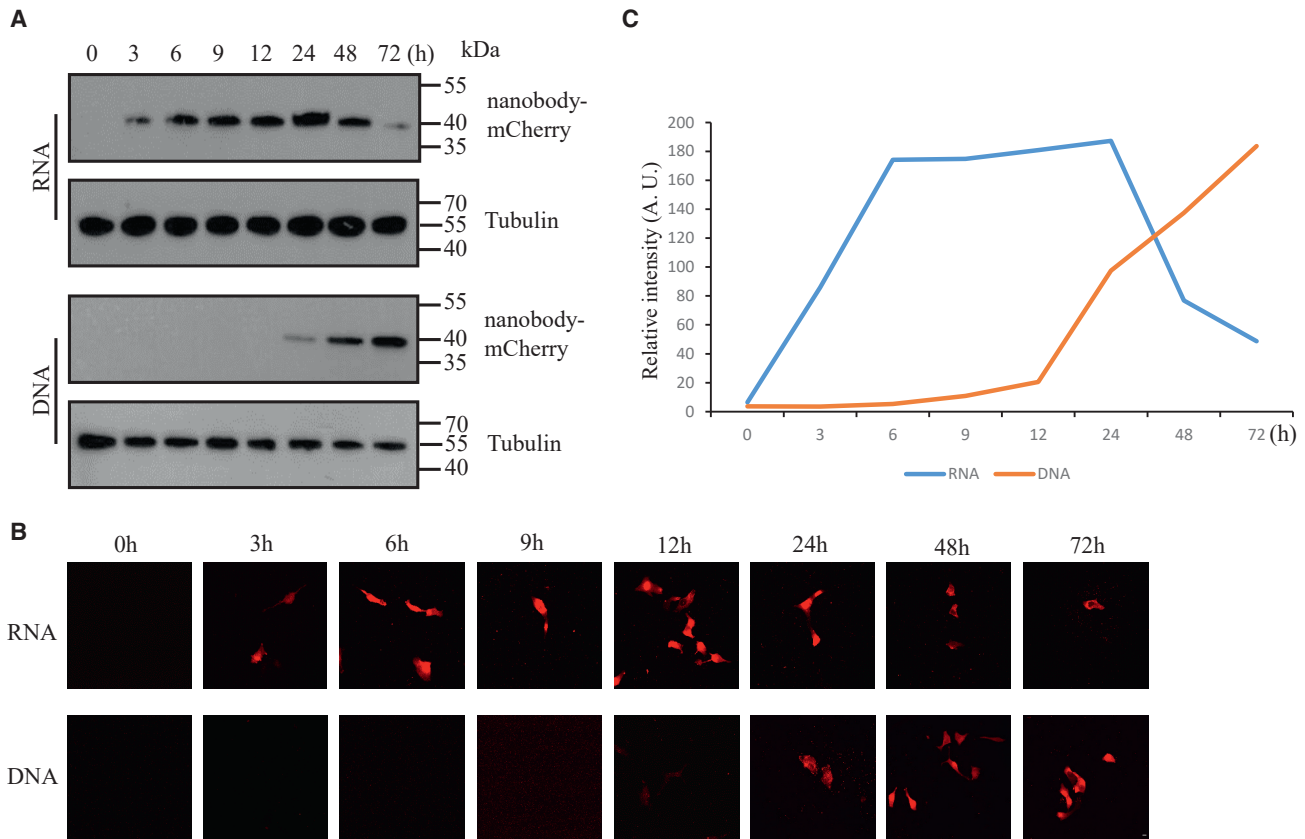
Figure 3. The Anti-GFP Nanobody-mCherry Expressed via IVT mRNA Produced and Degraded Earlier Than the pmCherry-N1/Nanobody in HeLa Cells

(A) Total cell extracts of the nanobody-mCherry expressed via mRNA and the plasmid from 0 h to 3 days were analyzed by western blots. The predicted size of the chimeric protein is 41 kDa (top panel). As a loading control, the blot was reincubated with an antibody against tubulin (bottom panel). (B) Time point comparison of the nanobody-mCherry expressed via mRNA and the plasmid both fused with a red fluorescent protein (mCherry) from 0 h to 3 days. Scale bar, 10 μm. (C) Summary graph showing a significant change in the relative fluorescence intensity of nanobody-mCherry expressed via RNA or DNA in a different time lapse. The data are shown as the mean ± SEM.

degraded mostly. Compared to IVT mRNA, the nanobody-mCherry expressed via the plasmid progressively produced from 24 h to 72 h and did not disappear at 72 h after transfection. The relative fluorescence intensity of the nanobody was shown in Figure 3C.

In A549 cells, the same results of Figure 3 were shown (Figure S1). A549 cells were also transfected with the same concentration of IVT mRNA and the plasmid. Western blot and microscopy analyses of transfected cells showed that the nanobody-mCherry expressed via IVT mRNA can be expressed at 3 h, peaked at 24 h, then degraded at 48 h, and disappeared mostly at 72 h after transfection. At the same time, the nanobody-mCherry expressed via the plasmid progressively produced from 24 h to 72 h and did not disappear at 72 h after transfection (Figures S1A and S1B). The relative fluorescence intensity of the nanobody was shown in Figure S1C. The relative fluorescence intensity of cells expressing the nanobody-mCherry was fitted to the phenomenon of Figure 3, in which the nanobody-mCherry expressed via IVT mRNA produced and degraded earlier than the plasmid.

Optimization IVT mRNA Construction for the Best Protein Production

To be efficiently translated, most eukaryotic mRNAs require a 7-methyl guanosine (m^7G) cap structure at the 5′ end and a poly(A) tail length of 300 nt at the 3′ end,[20] as well as UTRs.[21] We also allow for partial incorporation of 5-methyl-cytosine-5'-triphosphate (5mCTP), pseudo-UTP, and other modified nucleotides into mRNA, which abrogate mRNA interaction with Toll-like receptor (TLR)3, TLR7, TLR8, and retinoid-inducible gene I (RIG-I), resulting in low immunogenicity and higher stability in mice.[22]

In order to optimize the highest production and determine the mRNA function in the anti-GFP nanobody-mCherry translation, we produced four different mRNA mutations, such as no incorporation of 5mCTP and pseudo-UTP into mRNA, no UTRs (including 5′ and 3′ UTR) in T7 RNA polymerase templates, the poly(A) tail length of 150 nt at the 3′ end of mRNA, and no m^7G cap structure at the 5′ end of mRNA. They were termed as mRNA with nucleoside triphosphates (NTPs), mRNA with 5mCTP and pseudo-UTP without UTRs, mRNA with 5mCTP and pseudo-UTP with half poly(A) tail, and
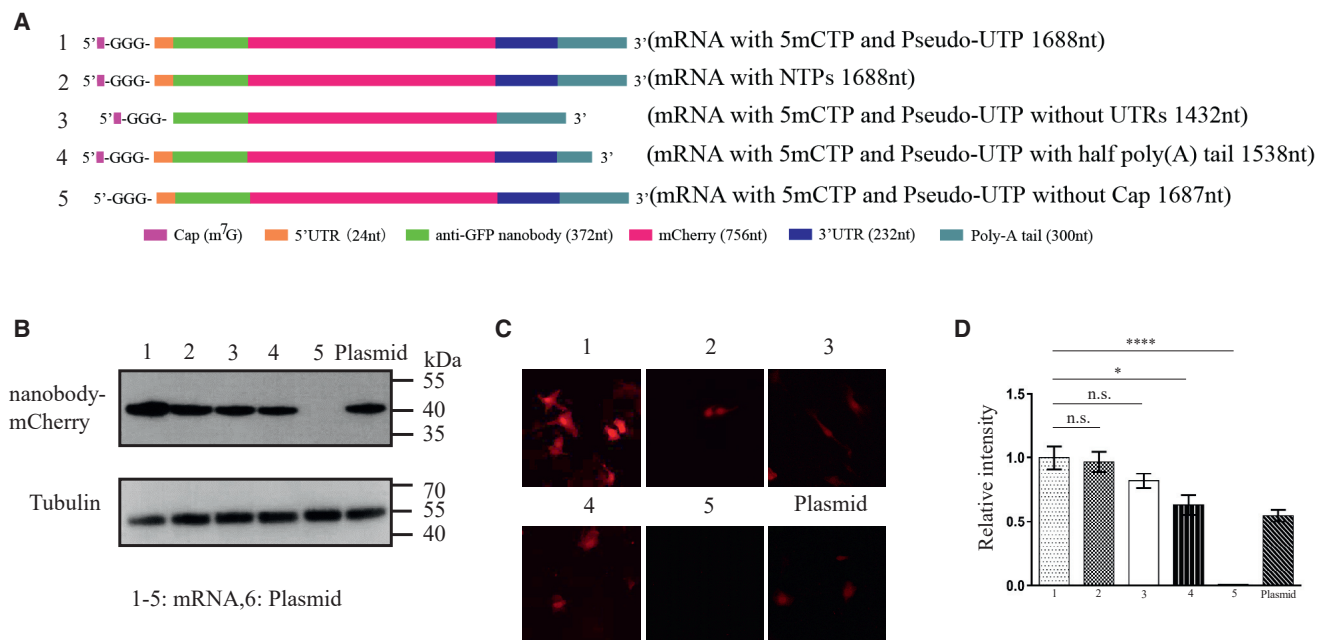
Figure 4. Setting IVT mRNA Construction for the Best Protein Production in HeLa Cells

(A) Structures of five different mRNAs after changing or removing one of the key components. (B) Total cell extracts of the nanobody-mCherry expressed via five different mRNAs, and plasmid were analyzed by western blots. The predicted size of the chimeric protein is 41 kDa (top panel). As a loading control, the blot was reincubated with an antibody against tubulin (bottom panel). (C) The anti-GFP nanobody-mCherry expressed via five different mRNAs and plasmid. Scale bar, 10 μm. (D) Summary graph showing a significant decrease in the relative fluorescence intensity of nanobody-mCherry in the four RNA mutants: 2, 3, 4, and 5 as shown in (A), compared with the 1 in (A). The data are shown as the mean ± SEM; asterisks indicate significant differences between the 1 in (A) and the four RNA mutants. $*p < 0.05$; $**p < 0.01$; $***p < 0.001$; n.s., not significant.

mRNA with 5mCTP and pseudo-UTP without 5′-cap, respectively (Figure 4A). The RNA length of mRNAs after tailing for 15 min (called half poly(A) tail) and 30 min (called mRNA) on an Agilent 2100 bioanalyzer was also shown (Figure S2).

In order to determine the proper amount of mRNA transfection, we compare different concentrations of the nanobody-mCherry expressed via mRNA fused with a red fluorescent protein (mCherry) from 0 to 2 μg per 10^6 cells. As the relative fluorescence intensity of the nanobody was shown in Figure S3B, production of the anti-GFP nanobody-mCherry expressed via IVT mRNA in 1.5 μg and 2 μg per 10^6 cells has reached the highest and is enough for transfection.

At 24 h after the same concentration of mRNAs and plasmid, the western blot and microscopy analyses of the nanobody-mCherry production showed significant results in HeLa cells (Figures 4B and 4C), whereas Figure 4D displays the relative fluorescence intensity of the top ten cells producing the nanobody-mCherry in Figure 4C. In conclusion, the relative fluorescence intensity of cells producing the nanobody-mCherry expressed via mRNA with NTPs decreased a little. The relative fluorescence intensity of cells producing the nanobody-mCherry expressed via mRNAs without UTRs and with half poly(A) tail decreased almost 20% and 40% and expressed via mRNA without 5′-cap was none. The relative fluorescence intensity

of cells producing the nanobody-mCherry expressed via plasmid was done as a control. It showed that the 5′-cap structure is crucial to protein production, and the poly(A) tail length of 300 nt, UTRs, and incorporation of modified nucleotides enhanced protein producing.

So far, we have constructed the most stable, efficient, and productive nanobody-mCherry expressed via IVT mRNA, such as anti-GFP, anti-vimentin, and anti-HDAC6 nanobodies. All of them can be rapidly, intracellularly transfected into different living cells to specifically target and trace cell skeletons, organelle, and cytoplasmic molecules.

DISCUSSION

The dramatic shift in the types of modified antibodies has been exposed in reaching clinical trial studies. There is a main focus on new advances in targeting antibodies to the central nervous system and intracellular compartments. However, their target repertoire is limited to few numbers of tumor-specific or associated cell-surface antigens. Intracellular molecules represent almost one-half of the human proteome and provide a broadly potential therapeutic target.[23] So antibodies have been developed into binding externalized antigens and have also been engineered to enter into cells or expressed intracellularly with the aim for combining intracellular antigens.

Intracellular antibodies are these antibodies which produce and bind antigens within the same cell. This is a different delivery strategy from antibodies produced extracellularly and engineered to penetrate cell membranes for accessing their intracellular targets. There are some strategies for targeting intracellular tumor antigens with antibody therapy. Antibodies can be fused to cell-penetrating peptides, which allow internalization of the antibody.[24–26] However, the approach achieving direct cytosolic protein delivery via modification with a cyclic peptide requires more manipulation.[27–29]

Plasmids or viral vectors can also be used to deliver antibody-encoding genes into the cell. Nanoparticles, dendrimers, or liposomes can be used to deliver an antibody or an expression vector encoding the intracellular antibody into the target cell. Recent advances on transcribed (IVT) mRNA in vitro have made it possible to deliver genetic information in many areas of intracellular research in living cells. Compared to intracellular delivery expressed by DNA, mRNA vaccines represent a promising alternative to conventional vaccine approaches due to their high potency, capacity for rapid development, as well as potency for low-cost manufacture and safe administration.[30,31] Plasmids need to be situated in the nucleus and then to be transcribed into mRNA, and their function depends on the cell cycle. Once IVT mRNA reaches the cytoplasm, the mRNA will be translated immediately, which may increase the transfection efficiency. In addition, IVT mRNA-based therapeutics, unlike plasmids, do not need to be integrated into the genome and do not have a risk of insertional mutation of genomics.[32] For most pharmaceutical applications, it is also an advantage that IVT mRNA is only transiently active and completely degraded via metabolic pathways.

In order to increase the stability of mRNA, there is an inclusion of chemically modified nucleotides.[33] (1) Kormann et al.[22] have shown that the replacement of only 25% of uridine and cytidine residues by 2-thiouridine and 5-methyl-cytidine suffices to increase mRNA stability, as well as to reduce the activation of innate immunity triggered by externally administered mRNA in vitro. (2) Another important feature influencing mRNA translation efficiency is the poly(A) tail, which is located on the 3′ end. It has been shown that a prolongation of the poly(A) tail to 120 nt has beneficial effects on protein expression, assumingly because of the protective effect of longer poly(A) tails; mRNAs with poly(A) tails shorter than 50 nt are claimed not to be translated at all.[20,34] (3) Capped mRNA can increase the translated efficiency. Standard cap analogs can be incorporated in either direction, resulting in only 50% of capped mRNA that is functional in protein translation. (4) On the other hand, UTRs in mRNAs have been reported to play a pivotal role in regulating both mRNA stability and mRNA translation. UTRs are known to influence translational initiation, elongation, and termination, as well as mRNA stabilization and intracellular localization through their interaction with RNA binding proteins.[35] Depending on the specific motives within the UTR, it can either enhance or decrease mRNA turnover.[21,36] Recently, data on mRNA half lives and the corresponding UTR sequences have been published.[37,38]

The antibody depicted on the diagram could represent a full-length immunoglobulin G (IgG), a Fab fragment, single-chain variable fragment (scFv), or a single domain antibody. As mentioned before, the nanobody/V_HH has an advantage in this field, representing the smallest intact antigen-binding fragment with an increased stability and solubility compared with those of conventional monoclonal antibodies. Caplacizumab,[39] anti- von Willebrand factor (vWF) nanobody/V_HH to treat acquired thrombotic thrombocytopenic purpura (aTTP), has the potential to become an important new component in the standard of care. KN035[40] is an anti-programmed death ligand 1 (PD-L1) nanobody/V_HH that can strongly induce T cell responses and inhibit tumor growth.

Here, we present a possibility of rapidly generating nanobodies/V_HHs in living cells to target intracellular antigens. The anti-GFP nanobody/V_HH expressed via IVT mRNA can recognize and trace F-actin-GFP and Golgi-GFP in skeleton and organelle compartments after transfection. We showed that nanobodies/V_HHs expressed via IVT mRNAs can efficiently and specifically target antigens. The anti-GFP nanobody-mCherry can be found as early as within 3 h after transfection with IVT mRNA, which was not found until 24 h after transfection with the pmCherry-N1/anti-GFP nanobody. Furthermore, the nanobody/V_HH expressed via IVT mRNA degraded as early as 48 h after transfection, which would not happen to the plasmid. Last, but not least, due to the inclusion of chemically modified nucleotides, UTRs, the poly(A) tail length of 300 nt, and the 5′-cap structure, it suffices to increase the stability of IVT mRNA and the production of the nanobody-mCherry. This research focused on the development of nanobodies/V_HHs delivered into living cells with IVT mRNAs for the first time. It is an essential step for the use of nanobodies/V_HHs in clinical study. Ultimately, the nanobodies/V_HHs expressed via IVT mRNAs are tools toward potentially any antigenic cellular structure, being available to make possible functional studies.

MATERIALS AND METHODS
Expression Plasmids and PCR Templates
Lifeact is a 17-amino acid peptide for staining F-actin structures in eukaryotic cells.[41] The DNA sequence of the peptide fused to the GFP was synthesized by GENEWIZ, and the construct was called F-actin-GFP. For targeting human Golgi-resident enzyme N-acetyl-galactosaminyltransferase 2,[42] a molecular probe called CellLight Golgi-GFP, BacMam 2.0, was purchased from Invitrogen. GFP-binding, vimentin-binding, and HDAC6-binding nanobody/V_HH DNA sequences were synthesized by GENEWIZ. The sequences of three nanobodies were shown in Figure S4. To test the distribution of three nanobodies/V_HHs in living cells, we fused them to a red fluorescent protein (mCherry) to generate three visible antibodies, and the sequences also used the vector pcDNA3.1 (+). The reconstructed plasmids were amplified by PCR using the following oligonucleotides: 5′-TAA TAC GAC TCA CTA TAG GGG AGA CCC AAG CTG GCT A-3′, 5′-AGA ATA GAA TGA CAC CTA CTC-3′ to generate PCR templates.

General Synthesis of Nanobodies/V$_H$Hs Expressed via IVT mRNAs

The ARCA was used. PCR templates containing a T7 promoter in the correct orientation can be transcribed using the HiScribe T7 ARCA mRNA kit (with tailing; NEB; #E2060S). PCR product should be purified and run on an agarose gel to confirm amplicon size prior to its use as a template in the T7 ARCA mRNA transcription reaction. Generally, 0.1–0.5 μg of PCR fragments can be used in a 20-μL *in vitro* transcription reaction. After the preparation of PCR templates, standard mRNA synthesis with modified nucleotides should be started with thawing the necessary kit components, mixing, and pulse spinning in a microfuge to collect solutions to the bottoms of the tubes. The reaction was assembled at room temperature in the following order: nuclease-free water (to 20 μL), 2 × ARCA/NTP mix (10 μL), 5mCTP (10 mM, 2.5 μL), pseudo-UTP (10 mM, 2.5 μL), template DNA (1 μg), and T7 RNA polymerase mix (2 μL); mixed thoroughly; and pulse spun in a microfuge. Incubation was at 37°C for 30 min. DNase treatment to remove template DNA included adding 2 μL of DNase I, mixing well, and incubating at 37°C for 15 min. poly(A) tailing starts with setting up the tailing reaction as below. Standard tailing reaction volume was 50 μL: H$_2$O (20 μL), IVT reaction (20 μL), 10 × poly(A) polymerase reaction buffer (5 μL), and poly(A) polymerase. It was mixed thoroughly, pulse spun in a microfuge, and incubated at 37°C for 30 min. Synthesized mRNA can be purified by LiCl precipitation, phenol/chloroform extraction, followed by ethanol precipitation. To the 50-μL tailing reaction, 25 μL LiCl solution was added and mixed well. Incubation at −20°C for 30 min was completed, as was centrifugation at 4°C for 15 min at top speed to pellet the RNA. The supernatant was removed carefully, the pellet was rinsed by adding 500 μL of cold 70% ethanol and centrifuged at 4°C for 10 min, ethanol was removed carefully, the tube was spun briefly to bring down any liquid on the wall, residual liquid was removed carefully using a sharp tip, the pellet was air dried, the mRNA was resuspend in 50 μL of 0.1 mM EDTA or a suitable RNA storage solution, and the RNA was heated at 65°C for 5–10 min to completely dissolve the RNA and mixed well.

Immunoblotting Analysis

In total, 100 ng of cell lysate transfected with the same concentration of DNA- or RNA-encoded, GFP-binding nanobody/V$_H$H was loaded onto a 12% SDS-PAGE gel. Separated proteins were transferred to a nitrocellulose (NC) membrane. Blots were blocked in Tris-buffered saline (TBS) with 0.1% Tween-20 (TBST) with 5% low-fat milk and incubated with 1.5 μg/mL anti-mCherry antibody and anti-tubulin antibody in TBST with 0.1% low-fat milk at 4°C. The membranes were then washed in TBST and incubated with a horseradish peroxidase (HRP)-conjugated goat anti-mouse IgG.

Cell Culture and Transfection and Image Analysis

The majority of the molecular biology, biochemistry, and cell biology reagents and chemicals used in this study was purchased from Sigma. Plasmid and RNA transfections were delivered via lipofection. Fetal bovine serum (FBS)-free medium was used during transfection to protect RNA from degradation. In addition, all of the consumables and reagents used in the experiment were RNase free. Cells were cultured on glass slides by using Dulbecco's modified Eagle's medium, supplemented with 10% fetal calf serum, 100 U/mL penicillin-streptomycin, and 100 U/mL L-glutamine at 5% CO$_2$ and 37°C. Slides were rinsed in phosphate-buffered saline (PBS), and cells were fixed in PBS with 4% paraformaldehyde (PFA) for 10 min. VectaShield (Vector Laboratories, Burlingame, CA, USA)-mounted microscopy slides were assessed with an LSM 710 confocal station (Zeiss).

ImageJ software (https://imagej.nih.gov/ij/; version 1.51) was used to quantify the fluorescence intensities. We set an arbitrary threshold based on the difference in intensity between the cells and the background regions. The sum of the pixels with intensities above the threshold was recorded by ImageJ. For comparison of fluorescence intensities among different samples, all samples were processed simultaneously and under identical conditions. For each samples, the top 10 highest fluorescence intensities of all cells were collected from 5 separate images. All statistical analyses were performed with a Mann-Whitney U test using GraphPad Prism 7. The methods used for the statistical analyses in all statistical graphs are described in the source data.

SUPPLEMENTAL INFORMATION

Supplemental Information can be found online at https://doi.org/10.1016/j.omtm.2020.01.008.

REFERENCES

1. Strohl, W.R. (2018). Current progress in innovative engineered antibodies. Protein Cell 9, 86–120.

2. Leavy, O. (2010). Therapeutic antibodies: past, present and future. Nat. Rev. Immunol. 10, 297.

3. Chan, A.C., and Carter, P.J. (2010). Therapeutic antibodies for autoimmunity and inflammation. Nat. Rev. Immunol. 10, 301–316.

4. Carter, P.J., and Lazar, G.A. (2018). Next generation antibody drugs: pursuit of the 'high-hanging fruit'. Nat. Rev. Drug Discov. 17, 197–223.

5. Trenevska, I., Li, D., and Banham, A.H. (2017). Therapeutic Antibodies against Intracellular Tumor Antigens. Front. Immunol. 8, 1001–1012.

6. Marschall, A.L., Frenzel, A., Schirrmann, T., Schüngel, M., and Dübel, S. (2011). Targeting antibodies to the cytoplasm. MAbs 3, 3–16.

7. Stocks, M. (2005). Intrabodies as drug discovery tools and therapeutics. Curr. Opin. Chem. Biol. 9, 359–365.

8. Muyldermans, S. (2001). Single domain camel antibodies: current status. J. Biotechnol. 74, 277–302.

9. Hamers-Casterman, C., Atarhouch, T., Muyldermans, S., Robinson, G., Hamers, C., Songa, E.B., Bendahman, N., and Hamers, R. (1993). Naturally occurring antibodies devoid of light chains. Nature 363, 446–448.

10. Zuo, J., Li, J., Zhang, R., Xu, L., Chen, H., Jia, X., Su, Z., Zhao, L., Huang, X., and Xie, W. (2017). Institute collection and analysis of Nanobodies (iCAN): a comprehensive database and analysis platform for nanobodies. BMC Genomics 18, 797.

11. Leslie, M. (2018). Small but mighty. Science 360, 594–597.

12. Rothbauer, U., Zolghadr, K., Tillib, S., Nowak, D., Schermelleh, L., Gahl, A., Backmann, N., Conrath, K., Muyldermans, S., Cardoso, M.C., and Leonhardt, H. (2006). Targeting and tracing antigens in live cells with fluorescent nanobodies. Nat. Methods 3, 887–889.

13. Costales, M.G., Matsumoto, Y., Velagapudi, S.P., and Disney, M.D. (2018). Small Molecule Targeted Recruitment of a Nuclease to RNA. J. Am. Chem. Soc. 140, 6741–6744.

14. Sahin, U., Karikó, K., and Türeci, Ö. (2014). mRNA-based therapeutics–developing a new class of drugs. Nat. Rev. Drug Discov. 13, 759–780.

15. Kubala, M.H., Kovtun, O., Alexandrov, K., and Collins, B.M. (2010). Structural and thermodynamic analysis of the GFP:GFP-nanobody complex. Protein Sci. 19, 2389–2401.

16. Maier, J., Traenkle, B., and Rothbauer, U. (2015). Real-time analysis of epithelial-mesenchymal transition using fluorescent single-domain antibodies. Sci. Rep. 5, 13402.

17. Herrmann, H., Bär, H., Kreplak, L., Strelkov, S.V., and Aebi, U. (2007). Intermediate filaments: from cell architecture to nanomechanics. Nat. Rev. Mol. Cell Biol. 8, 562–573.

18. Kawaguchi, Y., Kovacs, J.J., McLaurin, A., Vance, J.M., Ito, A., and Yao, T.P. (2003). The deacetylase HDAC6 regulates aggresome formation and cell viability in response to misfolded protein stress. Cell 115, 727–738.

19. Johnston, J.A., Ward, C.L., and Kopito, R.R. (1998). Aggresomes: a cellular response to misfolded proteins. J. Cell Biol. 143, 1883–1898.

20. Moore, M.J. (2005). From birth to death: the complex lives of eukaryotic mRNAs. Science 309, 1514–1518.

21. Mignone, F., Grillo, G., Licciulli, F., Iacono, M., Liuni, S., Kersey, P.J., Duarte, J., Saccone, C., and Pesole, G. (2005). UTRdb and UTRsite: a collection of sequences and regulatory motifs of the untranslated regions of eukaryotic mRNAs. Nucleic Acids Res. 33, D141–D146.

22. Kormann, M.S., Hasenpusch, G., Aneja, M.K., Nica, G., Flemmer, A.W., Herber-Jonat, S., Huppmann, M., Mays, L.E., Illenyi, M., Schams, A., et al. (2011). Expression of therapeutic proteins after delivery of chemically modified mRNA in mice. Nat. Biotechnol. 29, 154–157.

23. Cheever, M.A., Allison, J.P., Ferris, A.S., Finn, O.J., Hastings, B.M., Hecht, T.T., Mellman, I., Prindiville, S.A., Viner, J.L., Weiner, L.M., and Matrisian, L.M. (2009). The prioritization of cancer antigens: a national cancer institute pilot project for the acceleration of translational research. Clin. Cancer Res. 15, 5323–5337.

24. Freund, G., Sibler, A.P., Desplancq, D., Oulad-Abdelghani, M., Vigneron, M., Gannon, J., Van Regenmortel, M.H., and Weiss, E. (2013). Targeting endogenous nuclear antigens by electrotransfer of monoclonal antibodies in living cells. MAbs 5, 518–522.

25. Kimura, H., Hayashi-Takanaka, Y., Stasevich, T.J., and Sato, Y. (2015). Visualizing posttranslational and epigenetic modifications of endogenous proteins in vivo. Histochem. Cell Biol. 144, 101–109.

26. Prochiantz, A. (2000). Messenger proteins: homeoproteins, TAT and others. Curr. Opin. Cell Biol. 12, 400–406.

27. Sánchez-Navarro, M., Teixidó, M., and Giralt, E. (2017). Cytosolic delivery: Just passing through. Nat. Chem. 9, 727–728.

28. Dinca, A., Chien, W.M., and Chin, M.T. (2016). Intracellular Delivery of Proteins with Cell-Penetrating Peptides for Therapeutic Uses in Human Disease. Int. J. Mol. Sci. 17, 263–275.

29. Kristensen, M., Birch, D., and Mørck Nielsen, H. (2016). Applications and Challenges for Use of Cell-Penetrating Peptides as Delivery Vectors for Peptide and Protein Cargos. Int. J. Mol. Sci. 17, 185–201.

30. Pardi, N., Hogan, M.J., Porter, F.W., and Weissman, D. (2018). mRNA vaccines - a new era in vaccinology. Nat. Rev. Drug Discov. 17, 261–279.

31. Pastor, F., Berraondo, P., Etxeberria, I., Frederick, J., Sahin, U., Gilboa, E., and Melero, I. (2018). An RNA toolbox for cancer immunotherapy. Nat. Rev. Drug Discov. 17, 751–767.

32. Veiga, N., Goldsmith, M., Granot, Y., Rosenblum, D., Dammes, N., Kedmi, R., Ramishetti, S., and Peer, D. (2018). Cell specific delivery of modified mRNA expressing therapeutic proteins to leukocytes. Nat. Commun. 9, 4493–4501.

33. Karikó, K., and Weissman, D. (2007). Naturally occurring nucleoside modifications suppress the immunostimulatory activity of RNA: implication for therapeutic RNA development. Curr. Opin. Drug Discov. Devel. 10, 523–532.

34. Pichon, X., Wilson, L.A., Stoneley, M., Bastide, A., King, H.A., Somers, J., and Willis, A.E. (2012). RNA binding protein/RNA element interactions and the control of translation. Curr. Protein Pept. Sci. 13, 294–304.

35. Pesole, G., Grillo, G., Larizza, A., and Liuni, S. (2000). The untranslated regions of eukaryotic mRNAs: structure, function, evolution and bioinformatic tools for their analysis. Brief. Bioinform. 1, 236–249.

36. Barrett, L.W., Fletcher, S., and Wilton, S.D. (2012). Regulation of eukaryotic gene expression by the untranslated gene regions and other non-coding elements. Cell. Mol. Life Sci. 69, 3613–3634.

37. 't Hoen, P.A., Hirsch, M., de Meijer, E.J., de Menezes, R.X., van Ommen, G.J., and den Dunnen, J.T. (2011). mRNA degradation controls differentiation state-dependent differences in transcript and splice variant abundance. Nucleic Acids Res. 39, 556–566.

38. Sharova, L.V., Sharov, A.A., Nedorezov, T., Piao, Y., Shaik, N., and Ko, M.S. (2009). Database for mRNA half-life of 19 977 genes obtained by DNA microarray analysis of pluripotent and differentiating mouse embryonic stem cells. DNA Res. 16, 45–58.

39. Peyvandi, F., and Callewaert, F. (2016). Caplacizumab for Acquired Thrombotic Thrombocytopenic Purpura. N. Engl. J. Med. 374, 2497–2498.

40. Zhang, F., Wei, H., Wang, X., Bai, Y., Wang, P., Wu, J., Jiang, X., Wang, Y., Cai, H., Xu, T., and Zhou, A. (2017). Structural basis of a novel PD-L1 nanobody for immune checkpoint blockade. Cell Discov. 3, 17004–17015.

41. Riedl, J., Crevenna, A.H., Kessenbrock, K., Yu, J.H., Neukirchen, D., Bista, M., Bradke, F., Jenne, D., Holak, T.A., Werb, Z., et al. (2008). Lifeact: a versatile marker to visualize F-actin. Nat. Methods 5, 605–607.

42. Storrie, B., White, J., Röttger, S., Stelzer, E.H., Suganuma, T., and Nilsson, T. (1998). Recycling of golgi-resident glycosyltransferases through the ER reveals a novel pathway and provides an explanation for nocodazole-induced Golgi scattering. J. Cell Biol. 143, 1505–1521.